Preparation of onion-like multilayered particles comprising mainly poly(iso-butyl methacrylate)-block-polystyrene by two-step AGET ATRP

Kitayama, Yukiya ; Yorizane, Mika ; Kagawa, Yasuyuki ; Minami, Hideto ; Zetterlund, Per B. ; Okubo, Masayoshi

(Citation)
Polymer,50(14):3182-3187

(Issue Date)
2009-07-03

(Resource Type)
journal article

(Version)
Accepted Manuscript

(URL)
https://hdl.handle.net/20.500.14094/90000906

Preparation of Onion-like Multilayered Particles Comprising Mainly Poly(*iso*-butyl Methacrylate)-*block*-Polystyrene by Two-Step AGET ATRP

Yukiya Kitayama, Mika Yorizane, Yasuyuki Kagawa, Hideto Minami, Per B. Zetterlund, Masayoshi Okubo*

Department of Chemical Science and Engineering,
Graduate School of Engineering, Kobe University, Kobe 657-8501, Japan

Tel/Fax: +81-78-803-6161
E-mail address: okubo@kobe-u.ac.jp

Part of CCCXXVII the series "Studies on Suspension and Emulsion"

Keywords: particle, morphology, atom transfer radical polymerization (ATRP),

Abstract

Synthesis of multilayered composite polymer particles comprising mainly poly(*iso*-butyl methacrylate)-*block*-polystyrene (P*i*BMA-*b*-PS) has been carried out by use of two-step activator generated by electron transfer for atom transfer radical polymerization (AGET ATRP) in aqueous microsuspension. P*i*BMA-Br macroinitiator seed particles were prepared in the first step, followed by swelling with styrene and subsequent second step (seeded) polymerization. The blocking efficiency in the second step was found to be crucial with regards to the resulting particle morphology. A disordered sea-island morphology was obtained when the blocking efficiency was 47% (73% conversion), whereas a blocking efficiency of 61% (71% conversion) resulted in formation of multilayered particles. High blocking efficiency can be achieved by careful adjustment of the activation rate by proper choice of polymerization temperature and amount of reducing agent (ascorbic acid).

Introduction

Composite polymer particles find a variety of applications such as in coatings and impact-modifiers [1-3]. The performance of composite polymer particles strongly depends on the morphology, and consequently extensive research has been aimed at controlling particle morphology [4-15]. Multilayered particles have a highly complex morphology comprising an often relatively high number of alternating polymer layers. Multilayered particles containing dyes in each layer may possess useful properties for applications such as three-dimensional optical data storage in information technology and security data encryption. The incorporation of dyes in different phases of the material minimizes energy transfer in the recording medium, while a highly regular structure of the material provides high-resolution recording [16, 17].

Multilayered particles can be prepared by sequential seeded polymerizations [18, 19], although this is a tedious process. An alternative and entirely different synthetic route to

multilayered particles entails the initial preparation of micron-sized, monodisperse poly(methyl methacrylate) (PMMA)/polystyrene (PS) core-shell particles by seeded dispersion polymerization (SDP) of styrene (S) with PMMA seed particles in ethanol/water. These core-shell particles had a thermodynamically unstable morphology (kinetic as opposed to thermodynamic morphology control) [20, 21]. Swelling of the particles with a good solvent allowed formation of the thermodynamically stable morphology, a multilayered "onion-like" structure, which was "fixed" by subsequent evaporation of the solvent [22]. PMMA-*b*-PS or PMMA-*g*-PS, formed during the SDP, played an important role as compatibilizer during formation of the multilayered structure [23]. Such multilayered particles have also been prepared by slow evaporation of toluene from toluene droplets with dissolved PS-*b*-PMMA having similar block lengths (M_{PS} = 5.0 - 17.0 × 10^4 g/mol; M_{PMMA} = 5.4 - 16.8 × 10^4 g/mol; M_w/M_n = 1.04 - 1.19) [24].

In view of the above, one wonders whether it is possible to prepare multilayered particles in one single step, i.e. by combining the synthesis of block copolymer and polymer particles. Traditionally, block copolymer has been synthesized by living anionic polymerization [25]. However, anionic polymerization is difficult to apply to aqueous systems. On the other hand, controlled/living radical polymerization (CLRP) [26], developed in the past two decades, has been successfully applied to aqueous dispersed systems [27, 28], and is a powerful tool for block copolymer synthesis. Several CLRP methods have been developed, including nitroxide-mediated radical polymerization (NMP) [29, 30], atom transfer radical polymerization (ATRP) [31-34], reversible addition/fragmentation chain transfer (RAFT) polymerization [35-38], and organotellurium-mediated radical polymerization (TERP) [39-42].

In previous work, we succeeded for the first time in the preparation of multilayered particles comprising poly(*i*so-butyl methacrylate)-*block*-polystyrene (P*i*BMA-*b*-PS) directly in an aqueous medium by two step ATRP without post treatment, employing the ethyl 2-bromoisobutyrate / CuBr / 4,4'-dinonyl-2,2'-dipyridyl (dNbpy) initiator system [43, 44]. The first and second steps were, respectively, carried out by direct ATRP in miniemulsion of *i*so-butyl methacrylate (*i*BMA) and by

seeded polymerization (seeded ATRP) of S using poly(*i*BMA)-Br (P*i*BMA) macroinitiator seed particles. However, the polymerization rate (R_p) of S in the second step was very low (90% conversion in 96 h at 70˚C) and the reproducibility was fairly poor. This would be caused by the inevitable oxidation of Cu(I) to Cu(II) due to oxygen entering the system during the addition of S, which is a common problem when implementing direct ATRP in aqueous dispersed systems. The problem of Cu(I) oxidation can be circumvented by use of the activator generated by electron transfer (AGET) ATRP technique, recently developed by Matyjaszewski and coworkers [45]. In AGET ATRP, the initially present Cu(II) complex is reduced to Cu(I) complex (the activator) in situ by a reducing agent such as ascorbic acid. Thus, during the oxygen removal process prior to polymerization, only Cu(II) is present, not Cu(I), and oxidation is therefore not a concern, making AGET ATRP highly suitable for ATRP in aqueous dispersed systems [27, 28, 46-48].

In the present work, two-step AGET ATRP has been employed for the preparation of onion-like multilayered P*i*BMA-*b*-PS particles. The results have been analyzed with particular focus on how the blocking efficiency (i.e. the efficiency of block copolymer formation) affects the particle morphology.

Experimental part

Materials

S and *i*BMA were purified by distillation under reduced pressure in a nitrogen atmosphere. The water used in all experiments was obtained from Elix® UV (Millipore, Japan) purification system and had a resistivity of 18.2 MΩ·cm^{-1}. Ethyl 2-bromoisobutyrate (EB*i*B) (Tokyo Kasei Kogyo Co. Ltd., Tokyo, Japan), 4,4'-dinonyl-2,2'-dipyridyl (dNbpy) (Aldrich Chem Co. Ltd.), $CuBr_2$ (Nacalai Tesque Inc., Kyoto, Japan), ascorbic acid (Nacalai Tesque, Kyoto, Japan), Brij98 (Aldrich Chem Co. Ltd.), and *n*-tetradecyltrimethylammonium bromide (TTAB) (Tokyo Kasei Kogyo Co. Ltd., Tokyo, Japan) were used as received.

Preparation of PiBMA seed (macroinitiator) particles by first step AGET ATRP

The organic phase (EB*i*B 343 mg, 1.75 mmol; dNbpy 2.875 g, 3.5 mmol; *i*BMA 50 g, 350 mmol) was mixed with an aqueous (430 g) solution of $CuBr_2$ (785 mg, 3.5 mmol) and Brij98 (2.5 g), and stirred vigorously for 1 min at 5200 rpm using a homogenizer. After addition of an aqueous solution (1 g) of ascorbic acid (248 mg, 1.4 mmol), AGET ATRP was conducted in a glass reactor (TEM V-1000, Taiatsu Techno Corp., Tokyo, Japan) at 40˚C at a pressure of 2.0 atm under nitrogen atmosphere. The conversion was measured by gas chromatography (GC-18A, Shimadzu Co., Kyoto, Japan). The polymerization was stopped by bubbling air through the mixture.

Preparation of PiBMA-b-PS particles by second step AGET ATRP of styrene

After P*i*BMA-Br seed particles were swollen with S (50 g) at room temperature overnight, the emulsion (10 g) was transferred to a glass ampoule and degassed using several N_2/vacuum cycles, followed by addition of an aqueous (1 g) solution of ascorbic acid (5.62 mg, 31.9 μmol, 1.0 equivalent ratio to $CuBr_2$ including in this system). The emulsion was once again degassed with several N_2/vacuum cycles and sealed off under vacuum. Second step AGET ATRP was carried out in sealed glass tubes at 70˚C under a nitrogen atmosphere. An alternative procedure was employed to improve the blocking efficiency: An aqueous miniemulsion of S comprising 225 g water, 50 g S, 1.25 g Brij 98 and 2.5 g TTAB was prepared by ultrasonication for 10 min. This miniemulsion was subsequently added to the seed emulsion comprising P*i*BMA-Br seed particles, allowing the seed particles to swell with S for 2 h (the use of a S miniemulsion reduces the time required for swelling to occur compared to when simply adding S monomer to the seed emulsion). Second step AGET ATRP was carried out at 40˚C for 2 h, followed by at 70˚C for prescribed times, using an equivalent ratio of $CuBr_2$ to ascorbic acid of 0.8.

Molecular weight measurements

Number-average molecular weights (M_n), weight-average molecular weights (M_w), and molecular weight distributions (MWD) were measured by gel permeation chromatography (GPC) with two S/divinylbenzene gel columns (TOSOH corporation, TSKgel GMH_{HR}-H, 7.8 mm i.d. × 30 cm) using THF as eluent at 40˚C at the flow rate of 1.0 ml/min employing refractive index (TOSOH RI-8020/21) and ultraviolet detectors (TOSOH UV-8II). The columns were calibrated with six standard PS samples ($1.05 \times 10^3 - 5.48 \times 10^6$, $M_w/M_n = 1.01 - 1.15$). The theoretical molecular weight ($M_{n,th}$) was according to $M_{n,th}=\alpha[M]_0 M_M/[I]_0$, where α is the fractional conversion of monomer, M_M is the molecular weight of monomer, and $[M]_0$ and $[I]_0$ are the initial concentrations of monomer and initiator (alkyl halide), respectively.

Observation of particle morphology

The dried particles were stained with ruthenium tetraoxide (RuO_4) vapor at room temperature for 30 min in the presence of 1% RuO_4 aqueous solution, and subsequently embedded in an epoxy matrix, cured at room temperature for 24 h, and finally microtomed. Ultrathin cross-sections of 100 nm in thickness were observed with a Hitachi H-7500 transmission electron microscope (TEM) at a voltage of 100 kV.

Results and discussion

Preparation of PiBMA-Br seed particles

AGET ATRP of *i*BMA was carried out at 40˚C using Brij98 as colloidal stabilizer. The polymerization proceeded smoothly without induction period, with the conversion reaching approximately 80% in 3 h. The polymerization was not taken to conversions > 80% in order to minimize loss of livingness at high conversion.

Figure 1 shows the MWDs, M_n and M_w/M_n as functions of conversion. The MWDs shifted to higher molecular weight with increasing conversion (Figure 1a), and the experimental M_n agreed

very well with the theoretical values. The level of control was very good as evidenced by narrow MWDs with $M_w/M_n < 1.3$ (Figure 1b), in fact significantly better than obtained in our previous work using direct ATRP to prepare P*i*BMA-Br seed particles [43]. Thus, first step AGET ATRP was successfully employed to prepare micrometer-sized (1-3 μm) P*i*BMA-Br seed particles comprising well-defined polymer of high livingness.

Preparation of PiBMA-b-PS particles by second step AGET ATRP

Figure 2 shows the conversion-time plot for the second step AGET ATRP of S at 70 °C using P*i*BMA-Br seed particles. The polymerization proceeded smoothly, reaching 90% in 19 h. The polymerization rate was markedly higher than in our previous work using direct ATRP at the same temperature, where 96 h was required for the polymerization to proceed to 90% conversion [43]. The higher R_p was most likely mainly caused by the AGET ATRP resulting in a lower concentration of Cu(II) compared to the direct ATRP.

The particle morphology was examined by TEM analysis of ultrathin cross-sections of the composite particles at 90% conversion, revealing a disordered structure as opposed to a multilayered structure (Figure 3). This is in sharp contrast to the well-defined multilayered structure observed in our previous work under similar conditions using direct ATRP [43].

Figure 4a shows RI-detector derived MWDs of the original P*i*BMA-Br macroinitiator as well as the MWDs obtained in the seeded polymerization. It is apparent that a significant fraction of the macroinitiator is in fact not living, evidenced by the low molecular weight peak at $\log M \approx 4.4$ that remains even at high conversion, coinciding with the original macroinitiator peak. This is further reinforced by comparison of the RI- and UV-detector derived MWDs (Figure 4a). The low molecular weight peak (macroinitiator) comprises *i*BMA units that are "UV-invisible", and consequently the non-living fraction of the macroinitiator is not detected by the UV detector. The M_n values (from RI detector) increased with conversion, but were significantly higher than $M_{n,th}$

(Fig 4b; calculated based on the number of macroinitiator chains, living or not). This discrepancy cannot be explained by a portion of the macroinitiator being dead – that would not alter M_n as the total number of chains is unaffected (although M_w would increase) – although it does explain the increase in M_w/M_n with conversion. The first step AGET ATRP of *i*BMA proceeded with high livingness (Figure 1), and it can therefore be deduced that the main fraction of the dead macroinitiator was actually formed during the initial stage of the second step AGET ATRP of S.

Figure 5 shows the livingness during the second step AGET ATRP. The livingness was estimated by transforming the MWDs (RI- and UV-detector derived) to number distributions ($w(\log M)/M^2$) vs. M. The distributions were subsequently normalized such that the high molecular weight segments were exactly superimposed (reasonable considering that the high molecular weight portion of polymer would be successfully extended macroinitiator, and therefore the UV- and RI-responses would be proportional to one another). The number fraction of non-extended macroinitiator relative to the total number of chains was then simply obtained as the integral of the UV-derived number distribution divided by the RI-derived number distribution (blocking efficiency: macroinitiator livingness (the number fraction of P*i*BMA-*b*-PS) = 100 – percentage of non-extended macroinitiator (the number fraction of P*i*BMA). The livingness of the macroinitiator was approximately 72%, whereas the livingness during the seeded polymerization remained close to constant (blocking efficiency 47% at 73% conversion). Thus, the livingness decreased quite significantly during the early and/or initial stage of the seeded polymerization. The composite particles obtained therefore comprise a very significant amount of dead P*i*BMA in addition to the block copolymer (P*i*BMA-*b*-PS). It appeared likely that the block copolymer content was not sufficiently high for formation of multilayered particles, thus resulting in a disordered structure instead.

In our previous work [24], onion-like multilayered particles were prepared by evaporation of toluene from polymer/toluene droplets in SDS aqueous medium when the PS-*b*-PMMA (M_{PS} = 1.7×10^5 g/mol; M_{PMMA} = 1.68×10^5 g/mol)/PMMA (M_{PMMA} = 1.3×10^4 g/mol) ratio was 100/0 and

80/20 (w/w). However, when the homopolymer content was increased to 50/50 (w/w), a cylinder-like morphology was instead obtained. Theoretical and experimental work on polymer films comprising block copolymer have revealed that lamellar morphology is not obtained when the amount of homopolymer present exceeds some critical limit [49, 50]. This has also been observed for the morphologies of PS/PS-*b*-PMMA/PMMA composite particles formed by the solvent evaporation method from toluene droplets with dissolved the polymers [24] . The above studies cannot be directly compared with the present work mainly because the latter entails simultaneous block copolymer formation and morphology development. However, the results are qualitatively consistent with the present findings in the sense that if the homopolymer content is too high, multilayered particles are not obtained.

Improving the blocking efficiency

An important feature of the livingness vs. conversion plot in Figure 5 is that the livingness remained close to constant during the seeded polymerization. This suggests that the blocking efficiency (initiation) of the macroinitiator was poor, whereas the seeded polymerization itself (i.e. after the initiation) proceeded without major loss of livingness. It was speculated that low blocking efficiency was mainly caused by a high bimolecular termination rate at the very initial stage of the seeded polymerization due to the high activation rate coefficient of P*i*BMA-Br at 70˚C (k_{act} = 5.27 $M^{-1}s^{-1}$) [51].

In order to improve the blocking efficiency, the amount of ascorbic acid was reduced from 100% to 80% (relative to the initial molar amount of $CuBr_2$) in the seeded polymerization. This would lead to an increase in the ratio [$CuBr_2$]/[CuBr] in the droplets/particles, and consequently a lower propagating radical concentration and less termination. The blocking efficiency was slightly improved to 49% (81% conversion) using this approach, but sea-island morphology was nonetheless obtained.

An alternative approach was subsequently adopted, which entailed carrying out the seeded polymerization at 40 °C for the first 2 hrs, followed by the remainder of the polymerization at 70 °C as before. During the initial 2 hrs at 40 °C, the polymer end group would change from P*i*BMA-Br to P*i*BMA-S-Br, and k_{act} of the latter (PS-Br) is approximately 50 times lower than that of the former (P*i*BMA-Br) at 70 °C [52]. Using this approach, the blocking efficiency increased to 55 % (conversion 91%), resulting in the formation of a multilayered structure in the very outer shell region of the particles, whereas the interior still exhibited a sea-island structure.

Finally, the two strategies were employed simultaneously. A reduction in the amount of ascorbic acid would cause a reduction in the propagating radical concentration, i.e. a reduction in the polymerization rate. However, as shown in Figure 2, using this approach, the seeded polymerization proceeded to high conversion with a similar polymerization rate as before using the strategies, reaching 94% conversion in 16 h. This would be caused by the increase in polymerization rate afforded by the increased blocking efficiency (Figure 5), i.e. the increase in the macroinitiator concentration.

As shown in Figure 6, as anticipated, the size of the low molecular weight peak as well as M_w/M_n were markedly reduced using this strategy. Moreover, the blocking efficiency was significantly improved (61% at 71% conversion) (Figure 5) - the livingness was considerably higher than before (47% at 73% conversion).

The obtained composite polymer particles have a broad particle size distribution as shown in Figure 7(a). The number-average particle diameter (D_n) and coefficient of variation (C_V) were 2.6 μm and 40 %, respectively. TEM analysis of ultrathin cross-sections of the composite particles, which have a broad size distribution as shown in Figure 7(a), at 94% conversion (Figure 7(b)) reveals that “onion-like” multilayered particles had indeed been formed, demonstrating the importance of a sufficiently high blocking efficiency in the seeded polymerization.

Conclusions

Multilayered composite polymer particles comprising mainly P*i*BMA-*b*-PS have been prepared by two-step AGET ATRP employing ascorbic acid as reducing agent in aqueous microsuspension. The blocking efficiency, i.e. the number fraction of block copolymer formed in the second step AGET ATRP, was shown to greatly influence the morphology. When the blocking efficiency was too low (approximately 40%), a disordered sea-island morphology was obtained. Low blocking efficiency was attributed to an excessively high activation rate at the early stage of the seeded polymerization, resulting in extensive bimolecular termination. In order to increase the blocking efficiency, the activation rate was suitably reduced by lowering the polymerization temperature and reducing the amount of ascorbic acid. In this way, sufficiently high blocking efficiency for formation of multilayered morphology was obtained while maintaining a high polymerization rate.

Acknowledgements. This work was partially supported by a Kobe University Takuetsu-shita Research Project.

References

1. Huang MR, Peng QY, and Li XG. Chem. Eur. J. 2006;12:4341-4350.
2. Li XG, Sun J, and Huang MR. Progress in Chemistry 2007;19:787-795.
3. Li XG, Ma XL, Sun J, and Huang MR. Langmuir 2009;25:1675-1684.
4. Sundberg DC and Durant YG. Polym. React. Eng. 2003;11:379-432.
5. Okubo M, Yamada A, and Matsumoto T. J. Polym. Sci. Polym. Chem. Ed. 1980;16:3219-3228.
6. Okubo M, Ando M, Yamada A, Katsuta Y, and Matsumoto T. J. Polym. Sci. Polym. Lett. Ed. 1981;19:143-147.
7. Okubo M, Katsuta Y, and Matsumoto T. J. Polym. Sci. Polym. Lett. Ed. 1982;20:45-51.
8. Lee DI and Ishikawa T. J. Polym. Sci. Polym. Chem. Ed. 1983;21:147-154.
9. Min TI, Klein A, El-Aasser MS, and Vanderhoff JW. J. Polym. Sci. Polym. Lett. Ed. 1983;21:2845-2861.
10. Muroi S, Hashimoto H, and Hosoi K. J. Polym. Sci. Polym. Chem. Ed. 1984;22:1365-1372.
11. Cho I and Lee K-W. J. Appl. Polym. Sci. 1985;30:1903-1926.
12. Okubo M. Makromol. Chem., Macromol. Symp. 1990;35/36:307-325.
13. Sheu HR, El-Aasser MS, and Vanderhoff JW. J. Polym. Sci. Part A: Polym. Chem. 1990;28:653-667.

14. Kim SH, Yi GR, Kim KH, and Yang SM. Langmuir 2008;24:2365-2371.
15. Jeon SJ, Yi GR, Koo CM, and Yang SM. Macromolecules 2007;40:8430-8439.
16. Siwick BJ, Kalinina O, Kumacheva E, Millar RJD, and Noolandi J. J. Appl. Phys. 2001;90:5328-5334.
17. Pham HH, Gourevich I, Oh JK, Jonkman JEN, and Kumacheva E. Adv. Mater. 2004;16:516-520.
18. Okubo M, Takekoh R, and Sugano H. Colloid Polym. Sci. 2000;278:559-564.
19. Gourevich I, Field LM, Wei Z, Paquet C, Petukhova A, Alteheld A, and Kumacheva E. Macromolecules 2006;39:1449-1454.
20. Okubo M, Izumi J, and Takekoh R. Colloid Polym. Sci. 1999;277:875-880.
21. Okubo M, Takekoh R, and Izumi J. Colloid Polym. Sci. 2001;279:513-518.
22. Yorimitsu H, Wakabayashi K, Shinokubo H, and Oshima K. Bulletin of the Chemical Society of Japan 2001;74:1963-1970.
23. Okubo M, Takekoh R, and Saito N. Colloid Polym. Sci. 2003;281:945-950.
24. Okubo M, Saito N, Takekoh R, and Kobayashi H. Polymer 2005;46:1151-1156.
25. Szwarc M, Levy M, and Milkovich R. J. Am. Chem. Soc. 1956;78:2656-2657.
26. Braunecker WA and Matyjaszewski K. Prog. Polym. Sci. 2007;32:93-146.
27. Zetterlund PB, Kagawa K, and Okubo M. Chem. Rev. 2008;108:3747-3794.
28. Cunningham MF. Prog. Polym. Sci. 2008;33:365-398.
29. Georges MK, Veregin RPN, Kazmaier PM, and Hamer GK. Macromolecules 1993;26:2987-2988.
30. Hawker CJ, Bosman AW, and Harth E. Chem. Rev. 2001;101:3661-3688.
31. Wang J and Matyjazewski K. J. Am. Chem. Soc. 1995;117:5614-5615.
32. Kato M, Kamigaito M, Sawamoto M, and Higashimura T. Macromolecules 1995;28:1721-1723.
33. Kamigaito K, Ando T, and Sawamoto M. Chem. Rev. 2001;101:3689-3745.
34. Matyjaszewski K. Advances in Controlled/Living Radical Polymerization. Washington, DC: American Chemical Society, 2003.
35. Chiefari J, Chong YK, Ercole F, Krstina J, Jeffery J, Le TPT, Mayadunne RTA, Meijs GF, Moad CL, Moad G, Rizzardo E, and Thang SH. Macromolecules 1998;31:5559-5562.
36. Moad G, Rizzardo E, and Thang SH. Australian Journal of Chemistry 2005;58:379-410.
37. Moad G, Rizzardo E, and Thang SH. Aust. J. Chem. 2006;59:669-692.
38. Moad G, Rizzardo E, and Thang SH. Polymer 2008;49:1079-1131.
39. Yamago S, Iida K, and Yoshida J. J. Am. Chem. Soc. 2002;124:13666-13667.
40. Sugihara Y, Kagawa Y, Yamago S, and Okubo M. Macromolecules 2007;40:9208-9211.
41. Okubo M, Sugihara Y, Kitayama Y, Kagawa Y, and Minami H. Macromolecules 2009;42:1979-1984.
42. Yamago S. Journal of Polymer Science Part a-Polymer Chemistry 2006;44:1-12.
43. Kagawa Y, Minami H, Okubo M, and Zhou J. Polymer 2005;46:1045-1049.
44. Okubo M, Minami H, and Zhou J. Colloid Polym. Sci. 2004;282:747-752.
45. Min K, Gao H, and Matyjazewski K. J. Am. Chem. Soc. 2005;127:3825-3830.
46. Li W, Min K, Matyjaszewsski K, Stoffelbach F, and Charleux B. Macromolecules 2008;41:6387-6392.
47. Stoffelbach F, Griffete N, Bui C, and Charleux B. Chem. Commun. 2008:4807-4809.
48. Stoffelbach F, Tibiletti L, Rieger J, and Charleux B. Macromolecules 2008;41:7850-7856.
49. Tanaka H, Hasegawa H, and Hashimoto T. Macromolecules 1991;24:240-251.
50. Whitmore MD and Noolandi J. Macromolecules 1985;18:2486-2497.
51. Pintauer T, Braunecker W, Collange E, Poli R, and Matyjaszewski K. Macromolecules 2004;37:2679-2682.
52. Goto A and Fukuda T. Macromol. Rapid Commun. 1999;20:633-636.

Table 1

Number-average molecular weight (M_n), weight-average molecular weight (M_w) and M_w/M_n of P*i*BMA and P*i*BMA-*b*-PS measured by RI and UV detection from GPC.

	Mn ($\times 10^4$)	Mw ($\times 10^4$)	PDI
PiBMA-Br (RI)	2.5	3.1	1.3
PiBMA-b-PS (RI)	7.6	19	2.4
PiBMA-b-PS (UV)	11	21	1.8

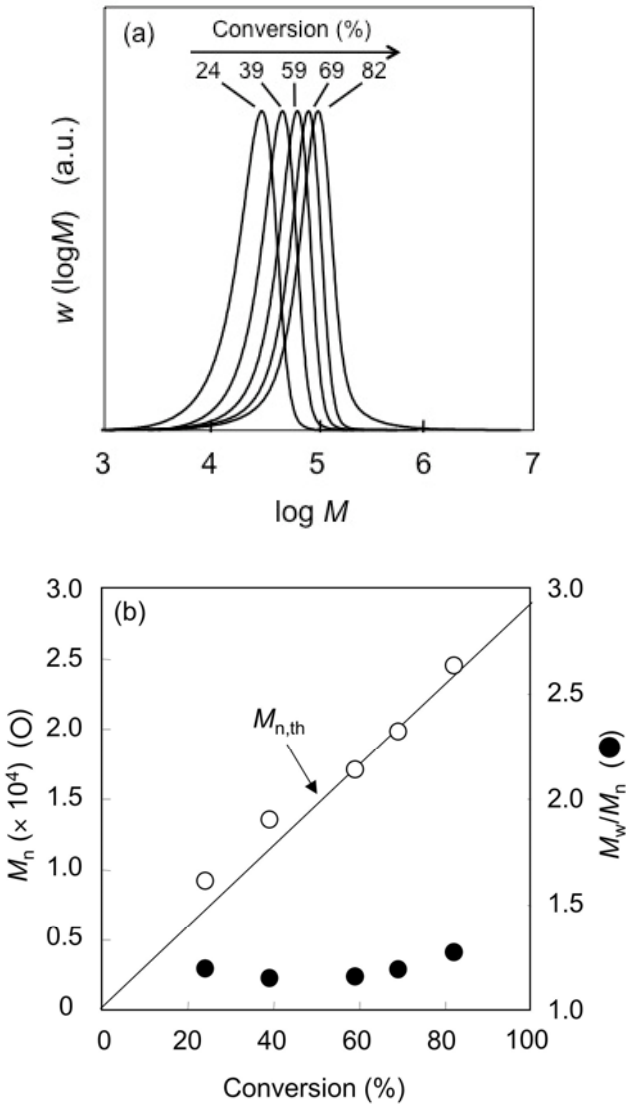

Fig. 1. MWDs (a), M_n and M_w/M_n (b) of P*i*BMA-Br prepared at various conversionsf of first step AGET ATRP of *i*BMA at 40˚C.

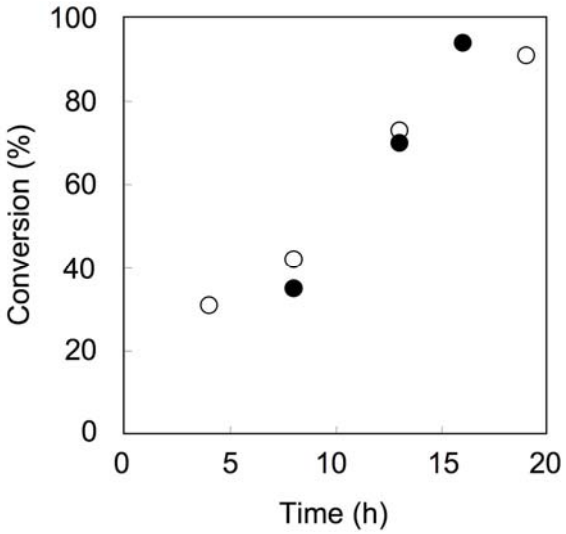

Fig. 2. Conversion vs time plots for second step AGET ATRP of S with P*i*BMA-Br seed particles at 70˚C (open circles), and 40˚C for 2 h, followed by 70˚C (closed circles). [$CuBr_2$]/[AsA] (equivalent ratio) = 1/1 (open circles) and 1/0.8 (closed circles).

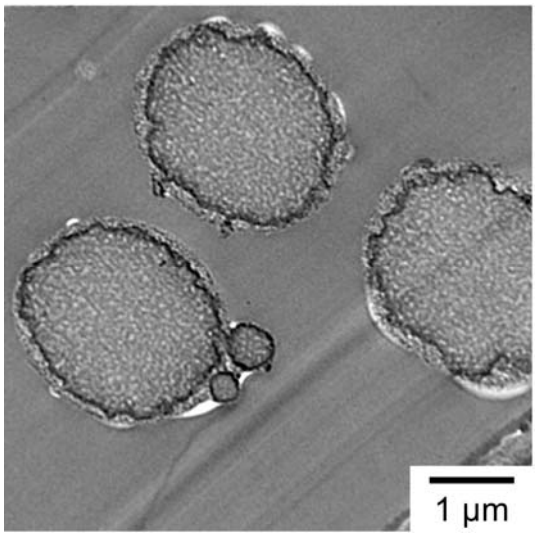

Fig. 3. TEM photograph of ultrathin cross sections of RuO_4-stained P*i*BMA-*b*-PS particles prepared by second step AGET ATRP at 70˚C (91% conversion). [$CuBr_2$]/[AsA] (equivalent ratio) = 1/1.

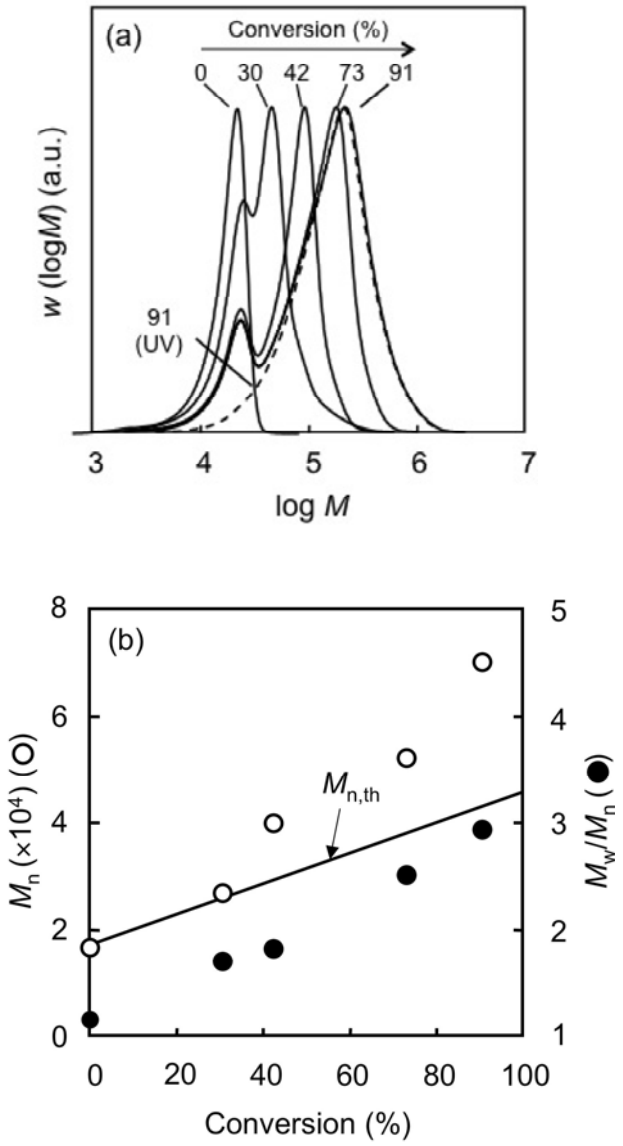

Fig. 4. MWDs (a), M_n (open circles) and M_w/M_n (closed circles) (b) of P*i*BMA-*b*-PS prepared at various conversions of second step AGET ATRP of S with P*i*BMA-Br seed particles at 70˚C. $[CuBr_2]/[AsA]$ (equivalent ratio) = 1/1. The full line and dashed line MWDs are attained from RI and UV detectors, respectively. Full line (b) is $M_{n,th}$.

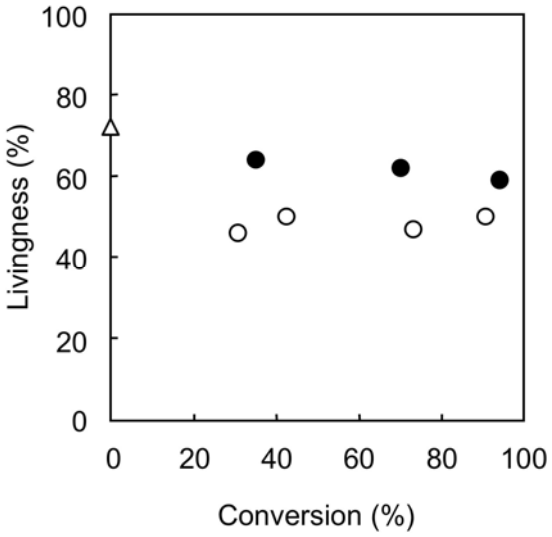

Fig. 5. Livingness as a function of conversion for seeded AGET ATRP of S with P*i*BMA-Br seed particles at 70˚C (open circles), and at 40˚C for 2 h followed by at 70˚C (closed circles). [$CuBr_2$]/[AsA] (equivalent ratio) = 1/1 (open circles) and 1/0.8 (closed circles). The triangle shows the livingness of the P*i*BMA macroinitiator.

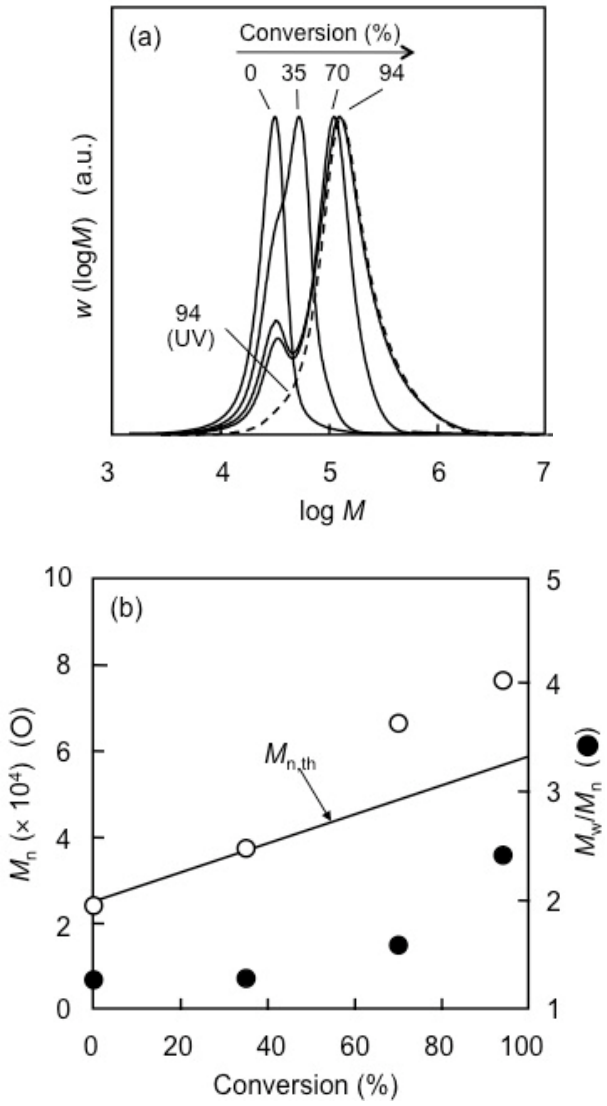

Fig. 6. MWDs (a) M_n (open circles) and M_w/M_n (closed circles) (b) of P*i*BMA-*b*-PS prepared at various conversions of seeded AGET ATRP of S with P*i*BMA seed particles at 40˚C for 2 h followed by 70˚C. $[CuBr_2]/[AsA]$ (equivalent ratio) = 1/0.8. The full line and dashed line MWDs are attained from RI and UV detectors, respectively. Full line (b) is $M_{n,th}$.

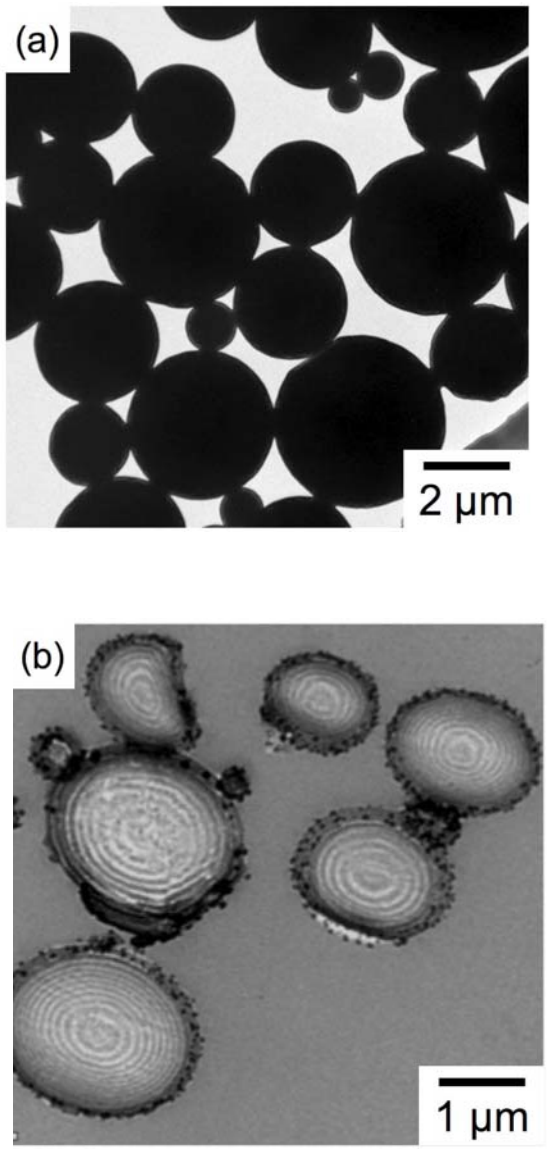

Fig. 7. TEM photograph of ultrathin cross-sections of RuO_4-stained P*i*BMA-*b*-PS particles prepared by seeded AGET ATRP of S using P*i*BMA-Br seed particles at 40˚C for 2 h followed by at 70˚C. $[CuBr_2]$/[AsA] (equivalent ratio: 1/0.8.